

## X-ray magnetic-circular-dichroism spectra on the superparamagnetic transition-metal ion clusters Mn12 and Fe8

P. Ghigna,<sup>1</sup> A. Campana,<sup>2</sup> A. Lascialfari,<sup>2</sup> A. Caneschi,<sup>3</sup> D. Gatteschi,<sup>3</sup> A. Tagliaferri,<sup>4</sup> and F. Borgatti<sup>5</sup>

<sup>1</sup>*Dipartimento di Chimica Fisica, Università di Pavia, V.le Taramelli 16, I-27100, Pavia, Italy*

<sup>2</sup>*Dipartimento di Fisica "A. Volta," Università di Pavia, Via Bassi 4, I-27100, Pavia, Italy*

<sup>3</sup>*Dipartimento di Chimica, Università di Firenze, Via Maragliano 75, I-50144, Florence, Italy*

<sup>4</sup>*ESRF Boîte Postale 220, F-38043 Grenoble Cedex, France*

<sup>5</sup>*INFM-OGG, c/o ESRF, Boîte Postale 220, F-38043 Grenoble Cedex, France*

(Received 31 July 2000; revised manuscript received 2 January 2001; published 13 September 2001)

X-ray magnetic-circular-dichroism (XMCD) spectra on the molecular superparamagnets  $[\text{Mn}_{12}\text{O}_{12}(\text{CH}_3\text{COO})_{16}(\text{H}_2\text{O})_{24}] \cdot 2\text{CH}_3\text{COOH} \cdot 4\text{H}_2\text{O}$  (in short Mn12) and  $[\text{Fe}_8\text{O}_2(\text{OH})_{12}(\text{tacn})_6]\text{Br}_2 \cdot 9\text{H}_2\text{O}$  (in short Fe8) are presented. The XMCD measurements have been performed at the Mn-L<sub>III,II</sub> edges in the Mn12 compound and at the Fe-L<sub>III,II</sub> edges in the Fe8 compound. For Fe8 the typical two-peak structure of Fe(III) compounds is found. For Mn12 and Fe8, from the dichroic signals a very low or negligible  $\langle L_z \rangle$  was obtained: to the best of our knowledge, this is the first direct experimental evidence of the quenching of the angular momentum by the crystal field in these systems. Quantitative analysis of the dichroic spectra for Fe8 yielded  $\langle L_z \rangle / \langle S_z \rangle = 0.02(1)$ .

DOI: 10.1103/PhysRevB.64.132413

PACS number(s): 75.50.Xx

$[\text{Mn}_{12}\text{O}_{12}(\text{CH}_3\text{COO})_{16}(\text{H}_2\text{O})_{24}] \cdot 2\text{CH}_3\text{COOH} \cdot 4\text{H}_2\text{O}$  (in short Mn12) and  $\text{Fe}_8(\text{tacn})_6$  (in short Fe8) are up to now the most accurately investigated systems presenting magnetic properties at molecular scale.<sup>1-3</sup> They are characterized by nonexchange-interacting unit molecules thus allowing the study of a bulk quantity as representative of the behavior of the single "finite-size" molecule. The structure of Mn12 can be described as formed by an external ring of 8 Mn(III) ions ( $S=2$ ) and an internal tetrahedron of four Mn(IV) ions ( $S=3/2$ ). The 12 Mn ions are strongly bound ferrimagnetically via the superexchange mechanism through oxygen bridges. As a result, the molecule behave as a magnetic cluster of spin  $S=10$ . This state can be loosely described setting all the Mn(III) ions with spin up ( $S=2 \times 8=16$ ), and all the Mn(IV) ions with spin down ( $S=-4 \times \frac{3}{2}=-6$ ). Fe8 has a typical butterfly structure, whereas the Fe(III)  $S=\frac{5}{2}$  ions are magnetically coupled through four main antiferromagnetic exchange constants. The total spin in the ground state is again  $S=10$ . The high-spin  $S=10$  ground state of these systems gives rise to spectacular superparamagnetic behaviors.<sup>1</sup> The crystal field splits the ground state in 21 energy levels characterized by the magnetic quantum number  $M_S$ . This ground-state structure gives an intrinsic bistability, which makes these systems interesting also for possible applications like, i.e., memory storage.

Although many different measurements have been performed on both compounds, still some problems remain open. Since in Mn12 manganese(III) ions are present, which in octahedral symmetry have a ground  ${}^5E_g$  state, orbital contributions to the magnetic moment cannot be excluded. Further it would be desirable to have a direct determination of the moments of the individual ions, in order to better establish the nature of the wave function of the magnetic ground state, which is important for modeling the mechanisms of thermal activation and quantum tunneling.<sup>1</sup>

Amongst the other techniques for characterizing the electronic structure and magnetic interactions, L-edge x-ray ab-

sorption spectroscopy is increasingly attracting attention:<sup>4</sup> the  $2p \rightarrow 3d$  transitions at the L edges are dipole allowed and strong, especially if compared to the weak dipole-forbidden (quadrupole allowed)  $1s \rightarrow 3d$  transitions characteristic of the K edges. In addition L-edges have smaller natural line-widths and the possibility of a strong magnetic circular dichroism effect.<sup>5</sup> In this work x-ray magnetic circular dichroism (XMCD) spectra of the molecular superparamagnets Mn12 and Fe8, at the Mn-L<sub>II,III</sub> and Fe-L<sub>II,III</sub>, respectively, are presented. The main interest of such a kind of measurements is that they give information about the ground-state magnetic moments, noticeably the orbital and spin-magnetic moments. The values of the moments can be obtained in the general case through the comparison of the experimental data with *ab initio* ionic multiplet calculations. However quite-simple sum rules exist<sup>6,7</sup> that allow to determine directly from the data the orbital moment. Even a spin-moment sum rule exists that is less general than the orbital one.<sup>7</sup> It requires the final-state spin-orbit splitting to be large enough to completely separate the L<sub>III</sub> and L<sub>II</sub> edges contributions. This limits its applicability to the Fe8 case. In addition, the  $2p$  core hole formed in final state of a L<sub>II,III</sub> edge x-ray absorption spectra interacts via Coulomb and exchange interactions with the  $3d$  valence electrons, thus making this technique sensitive to the oxidation state. Thus, in principle, the contributions of Mn(IV) and Mn(III) to the magnetic moment of Mn12 can be separated.

Mn12 was synthesized according to the literature method.<sup>2</sup> Crystals were obtained by vapor diffusion of acetone in the reagent solution; they were filtered and washed with acetone and identified by elemental-analysis technique. Fe8 was prepared by following the original-literature method.<sup>3</sup> Crystals were isolated by filtration after 2 weeks of slow evaporation of the solution and identified by elemental analysis. The XMCD spectra have been collected at the ID12B Dragon beamline at the European Synchrotron Radiation Facility (ESRF, Grenoble, France), in the total electron

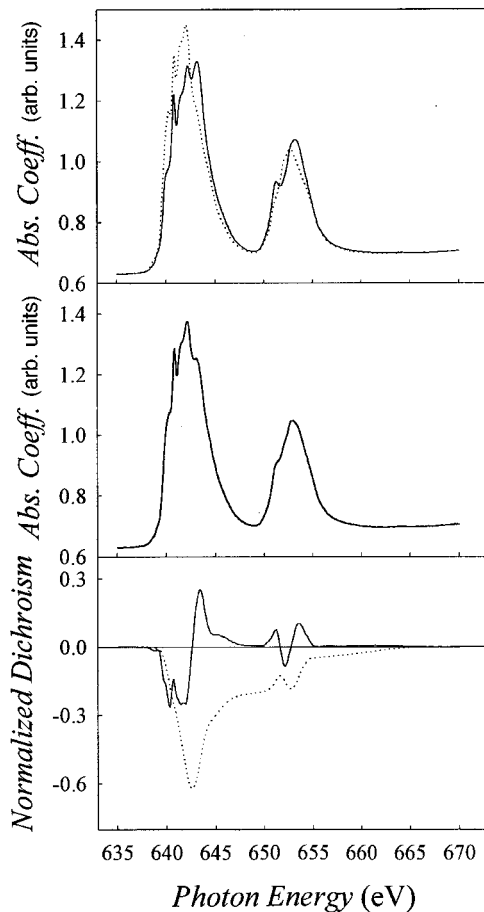


FIG. 1. Mn- $L_{II,III}$  edge XAS spectra of Mn12 at 5 K and in a field of 5 T, the dotted and full lines correspond to the two different photon helicities (upper panel). In the middle panel the isotropic spectrum is shown, as obtained from the average of the above two spectra. Lower panel: Mn- $L_{II,III}$  edge XMCD spectrum of Mn12 at 5 K and in a field of 5 T (full line), after normalization to 100% polarization rate and unit intensity of the peak in the isotropic XAS spectrum at ca. 642 eV. The dotted line is the running integral of the XMCD signal.

yield mode, which probes nearly a 25–50 Å layer for Fe metal at the energy of the  $L_{II,III}$  edges. The degree of circular polarization can be estimated to be near 85%.<sup>8</sup> For the experiment the samples have been mixed with an almost-equivalent amount (by volume) of graphite, ground in an agate mortar and then pressed to pellets. Each pellet has been then fixed to an aluminum sample holder by means of tantalum wires to ensure a proper electrical contact, and then transferred to the cold finger of a liquid-helium cryomagnet, which was kept under ultrahigh vacuum ( $10^{-10}$  mbar). The energy resolution was set to 0.2 eV by adjusting the entrance slits. The measurements have been taken in the 4–100 K temperature range and at different applied magnetic fields in the range 0.5–7 T. A correction was applied for incomplete light polarization. The measurements have demonstrated to be quite difficult due to sample degradation in the beam, the more sensitive material being Mn12. To minimize the effects of sample degradation we moved the sample with respect to the beam after a few dichroism scans, and periodically

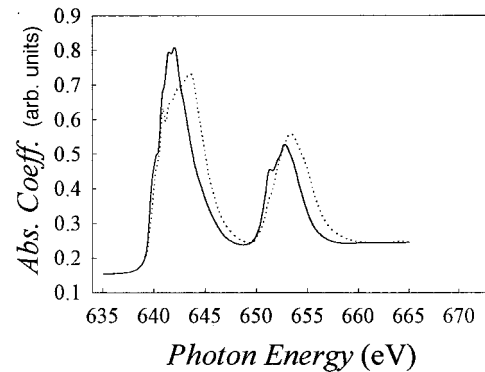


FIG. 2. Isotropic Mn- $L_{II,III}$  edge XAS spectra of  $Mn_2O_3$  (full line) and  $MnO_2$  (dotted line) at room temperature.

changed the sample; in addition, between each scan at fixed  $T$  and  $H$ , a valve was closed to avoid damaging the sample during the change of the experimental conditions. The lifetime of the sample exposed to a beam flux of  $10^{10}$  photon/sec can be estimated to be 3 and 4 h for Mn12 and Fe8, respectively.  $Mn_2O_3$  and  $MnO_2$  (Aldrich 99.99%) have been used as reference compounds for Mn(III) and Mn(IV), respectively.

Figure 1 shows (upper panel) the Mn- $L_{II,III}$  edge spectra of Mn12 taken with two opposite helicities, at 5 K and in a field of 5 T. In the middle panel the unpolarized absorption spectrum is shown, as obtained from the average of the previous spectra. For comparison, in Fig. 2 the Mn- $L_{II,III}$  edge absorption spectra of  $Mn_2O_3$  and  $MnO_2$  are shown. These two spectra display the well-known chemical shift of the absorption edges, according to which the spectral features are shifted to higher energy at higher-oxidation states; this can be explained in terms of the screening by the valence electrons of the Coulomb interaction between the  $2p$  initial states and the nucleus. The XMCD spectrum, obtained by the difference between the two spectra of the upper panel of Fig. 1 and normalizing at unit intensity of the peak at ca. 642 eV, is shown in the same Fig. 1 (lower panel).

The interpretation of XMCD signals at the  $L_{III-II}$  edges of a  $3d$  metal compound is generally not trivial, as the spectral shape changes drastically with either the strength of the crystal field or the relative magnitudes of the exchange and  $3d$  spin-orbit interactions.<sup>9–12</sup> However, there are a number of considerations that can be made in this case. For  $Mn_2O_3$  the  $L_{III}$  edge peaks near 642 eV, while for  $MnO_2$  the  $L_{III}$  edge peaks near 643.5 eV. Therefore, for Mn12, on the basis of the comparison with the spectra of the manganese oxides, the structures at the  $L_{III}$  edge close to ca. 642.5 eV can be ascribed mainly to Mn(III) states, while the structures close to ca. 643.5 eV can be ascribed as mainly due to Mn(IV) states. Although multiplet structure makes the spectra quite complicated, this unbalance of the spectral weight at different energies can be used, in principle, to disentangle the contribution of the two manganese sites by comparing with multiplet calculations. This would give a deeper understanding of the magnetic properties of manganese at the two sites, like, for example, the antiferromagnetic coupling. We want to point out that the above mentioned approach is quite deli-

cate and needs the knowledge of the local symmetries at the two sites together with very good reference spectra for the Mn(III) and Mn(IV) ions. From this point of view the  $\text{Mn}_2\text{O}_2$  and  $\text{MnO}_2$  samples seem not suitable enough showing no chemical shift at the onset of the  $L_{\text{III}}$  and  $L_{\text{II}}$  edges, although a shift of 1–1.5 eV of the main features is present at both edges. This can be attributed to the high degree of covalency of the Mn(IV)-O bond.

According to Thole *et al.*,<sup>6</sup> a sum rule states that the integral of the XMCD signal over a complete core-level edge is directly proportional to the expectation value of the orbital angular momentum in the ground state  $\langle L_z \rangle$ . In the case of spin-orbit split edges like the  $L_{\text{II,III}}$  the integral has to be taken over the two components: in the presence of an external magnetic field strong enough to magnetically saturate the sample, letting  $A$  and  $B$  to be the integrals of the dichroic signal under the  $L_{\text{III}}$  and  $L_{\text{II}}$  edges, respectively, the orbital part of the magnetic moment  $M_L$  is equal to  $-(2\mu_B/3C) \times [A+B]$ .  $C$  can be evaluated from the integral of the non-polarized spectrum, once the number of holes in the  $3d$  shell is known.<sup>4,6</sup> The integral curve of the XMCD spectrum of Fig. 1 is shown in the same figure as a dotted line. It is clearly apparent that the integral vanishes at the end of the spectrum. This gives the first direct experimental confirmation of the quenching of the orbital momentum by the crystal field in the Mn12 molecule. As it will be made more explicit later, the Mn edges cannot be clearly separated, nor the exact number of holes is known in this system. Nonetheless, it is worth noticing that the above conclusion of a complete quenching of the orbital momentum by the crystal field in Mn12 is independent of these difficulties as it is completely determined by the vanishing value of the integral of the dichroic signal.

The Fe- $L_{\text{II,III}}$  edge spectra of Fe8 taken with two opposite photon helicities are shown in Fig. 3, for a field of 7 T and at  $T=4$  K (upper panel). The middle panel of the same figure shows the unpolarized absorption spectrum, as obtained from the average of the previous spectra. High-spin Fe(III) ( $d^5$ ) in  $O_h$  symmetry has an  ${}^6A_1$  ground state, for which there is no first-order spin-orbit splitting. For this reason the overall shape of the absorption spectrum depends only on the crystal-field splitting  $10Dq$ ,<sup>9</sup> which in octahedral Fe(III) compounds with Fe-O or Fe-N coordination is close to 2 eV.<sup>10</sup> Therefore, the absorption spectrum shows a characteristic two-peak structure<sup>9</sup> that was already found in a number of compounds in which Fe(III) is in an octahedral environment.<sup>11–13</sup> The corresponding dichroism, obtained from the difference of the two spectra of the upper panel of Fig. 3 and after normalization at unit intensity of the peak at c.a. 710 eV, is shown in the same Fig. 3 (lower panel). The integral curve of the dichroic signal is also shown in Fig. 3 as a dotted line. The integral becomes small at the end of the spectrum, and we explain also in the Fe8 case the quenching of the angular momentum as a crystal-field effect.

Another useful sum rule allows to extract the ground-state expectation value of the spin momentum  $\langle S_z \rangle$  from the difference between the integrals of the dichroism over two spin-orbit split edges:<sup>7</sup> the spin part of the magnetic moment  $M_s$  equals  $-(\mu_B/C) \times [A-2B]$ , neglecting the intra-atomic

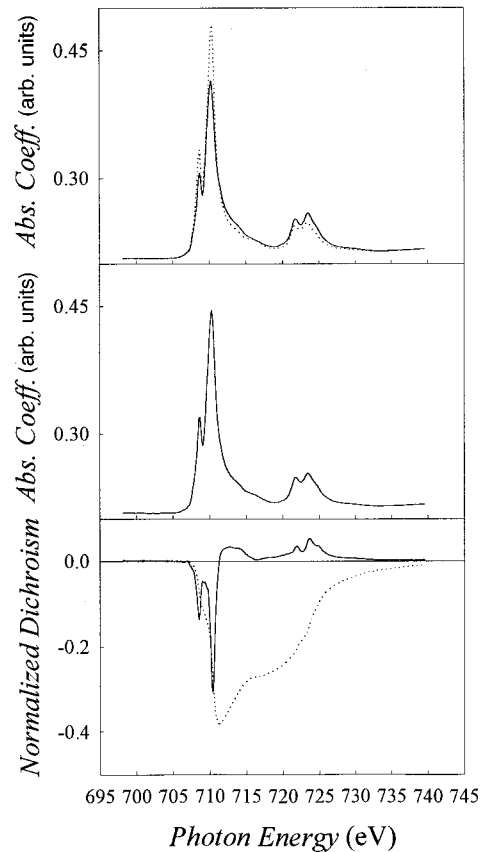


FIG. 3. Fe- $L_{\text{II,III}}$  edge XAS spectra of Fe8 at 4 K and in a field of 7 T; the dotted and full lines correspond to the two different photon helicities (upper panel). In the middle panel the isotropic spectrum is shown, as obtained from the average of the above two spectra. Lower panel: Fe- $L_{\text{II,III}}$  edge XMCD spectrum of Fe8 at 4 K and in a field of 7 T (full line), after normalization to 100% polarization rate and unit intensity of the peak in the isotropic XAS spectrum at ca. 710 eV. The dotted line is the running integral of the XMCD signal.

magnetic dipole moment.<sup>4,7</sup> In the case of the Mn- $L_{\text{II,III}}$  edges, the spin-orbit coupling is too weak, the  $L_{\text{II}}$  and the  $L_{\text{III}}$  states are mixed, and the spin momentum cannot be extracted reliably from the dichroic signal. However, this effect is negligible ( $<5\%$ ) at the end of the  $3d$  series,<sup>7</sup> and the separation can be done quite reasonably for Fe, for which the spin-orbit coupling is sufficiently large. At  $T=4$  K and  $H=7$  T for Fe8, using the ideal number of holes of 5 for a  $d^5$ Fe(III) atom, we found  $M_s=1.14$  in  $\mu_B$  units per Fe atom, which would yield a total magnetic spin momentum of  $9.12 \mu_B$ , to be compared with the value of  $20\mu_B$  one has to expect for the  $S=10$  ground state. In performing the calculation the border between the dichroism from the  $L_{\text{III}}$  and  $L_{\text{II}}$  edges was arbitrarily set at 716 eV, and this arbitrariness is of course a source of error. However, this error can easily be evaluated by varying the position of the border. The result is that, even using a very large interval, i.e., between 712 and 723 eV, the maximum deviation in  $M_s$  is around 15%. Therefore, the loss in magnetic moment that is found by XMCD is physical: one possible source can be the transfer of spin density from the metal to the ligand ions. As a matter of fact, a

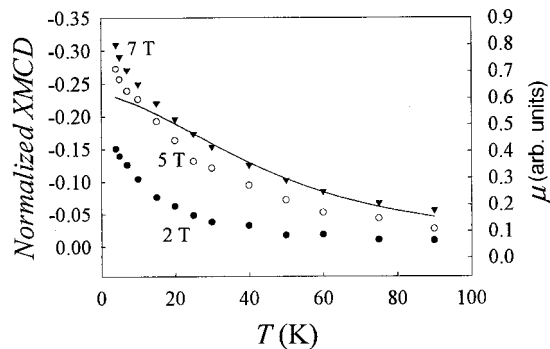


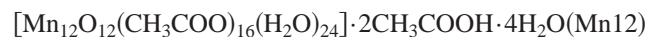
FIG. 4. Normalized XMCD intensity for the peak at 710 eV in the Fe8 compound at the indicated  $H$  and as a function of  $T$ . The line shows on an arbitrary scale the trend with  $T$  of total magnetic moment at 7 T.

very recent polarized-neutron-diffraction study performed on Mn12 showed reduced moments on all the inequivalent Fe sites.<sup>14</sup> Moreover, a nuclear magnetic resonance study<sup>15</sup> showed the existence of an important contact hyperfine interaction at the Fe sites, thus confirming the partial delocalization of the spin density on the ligand orbitals. However, this effect alone cannot explain the above huge difference: similar results in the  $\text{Cs}[\text{NiCr}(\text{CN})_6] \cdot 2\text{H}_2\text{O}$  molecular magnet have been attributed to incomplete magnetization originated from surface effects.<sup>16</sup> The trend with temperature and field of the intensity of the peak at ca. 710 eV in the dichroism is shown in Fig. 4; for comparison, in the same figure the trend with  $T$  of total magnetic moment in a field of 7 T is shown on an arbitrary scale as a full line. It is clearly apparent that while the magnetic moment saturates at low  $T$ , the dichroic signal never saturates; this is a clear indication that,

(likely, as for  $\text{Cs}[\text{NiCr}(\text{CN})_6] \cdot 2\text{H}_2\text{O}$ , due to surface effects) XMCD is in this case sensitive just to a fraction of the total magnetization.

Whatever the cause of this loss of magnetization detected by XMCD, it should be noticed that the measured value for the ratio between orbital and spin moments,  $\langle L_z \rangle / \langle S_z \rangle = 4(A+B)/3(A-2B)$  is not expected to be affected to a large extent, as incomplete magnetization effects are due to compensate. In addition  $C$  is eliminated and this avoids further uncertainties due to the inaccurate knowledge of the number of holes. We found  $\langle L_z \rangle / \langle S_z \rangle = 0.02(1)$ : this figure further supports the conclusion of an (almost) complete quenching of the orbital momentum in this system. The error has been evaluated as described above by letting the border between the dichroism from the  $L_{\text{III}}$  and  $L_{\text{II}}$  edges to float between 712 and 723 eV.

In summary, we have presented the first x-ray magnetic circular dichroism (XMCD) spectra on the molecular superparamagnets



and  $[\text{Fe}_8\text{O}_2(\text{OH})_{12}(\text{tacn})_6]\text{Br}_2 \cdot 9\text{H}_2\text{O}(\text{Fe8})$ , at the Mn- $L_{\text{II,III}}$  and at the Fe- $L_{\text{II,III}}$  edges, respectively. The main result of this investigation is the direct experimental confirmation of the quenching of the orbital momentum by the crystal field in both the compounds. For Fe8 the value of the ratio  $\langle L_z \rangle / \langle S_z \rangle$  extracted from the dichroic signal is as small as 0.02(1).

This work has been supported by the ESRF (Experiment HE-651). N. B. Brookes and S. S. Dhese are gratefully acknowledged for help during the x-ray absorption spectroscopy (XAS) data collection and for helpful discussions of the results.

<sup>1</sup>L. Thomas, F. Lioni, R. Ballou, D. Gatteschi, R. Sessoli, and B. Barbara, *Nature (London)* **383**, 145 (1996); C. Sangregorio, T. Ohm, C. Paulsen, R. Sessoli, and D. Gatteschi, *Phys. Rev. Lett.* **78**, 4645 (1997).

<sup>2</sup>T. Lis, *Acta Crystallogr., Sect. B: Struct. Crystallogr. Cryst. Chem.* **36**, 2042 (1980).

<sup>3</sup>K. Wiegardt, K. Pohl, I. Jibril, and G. Huttner, *Angew. Chem. Int. Ed. Engl.* **23**, 77 (1984).

<sup>4</sup>See, for example, J. Stöhr and R. Nakajima, *IBM J. Res. Dev.* **42**, 73 (1998), and references therein.

<sup>5</sup>G. van der Laan and B. T. Thole, *Phys. Rev. B* **42**, 6670 (1990).

<sup>6</sup>B. T. Thole, P. Carra, F. Sette, and G. van der Laan, *Phys. Rev. Lett.* **68**, 1943 (1992).

<sup>7</sup>P. Carra, B. T. Thole, M. Altarelli, and X. Wang, *Phys. Rev. Lett.* **70**, 694 (1993).

<sup>8</sup>M. Drescher, G. Snell, U. Kleineberg, H.-J. Stock, N. Müller, U. Heinzmann, and N. B. Brookes, *Rev. Sci. Instrum.* **68**, 1939 (1996).

<sup>9</sup>G. van der Laan and B. T. Thole, *Phys. Rev. B* **43**, 13 401 (1991).

<sup>10</sup>A. B. P. Lever, *Inorganic Electronic Spectroscopy* (Elsevier, Amsterdam, 1984).

<sup>11</sup>P. Kuiper, B. G. Searle, P. Rudolf, L. H. Tjeng, and C. T. Chen, *Phys. Rev. Lett.* **70**, 1549 (1993).

<sup>12</sup>G. Peng, J. Van Elp, H. Jang, L. Que, Jr., W. H. Armstrong, and G. Huttner, *J. Am. Chem. Soc.* **117**, 2515 (1995).

<sup>13</sup>E. Pellegrin, M. Hagelstein, S. Doyle, H. O. Moser, J. Fuchs, D. Vollath, S. Schuppler, M. A. James, S. S. Saxena, L. Niesen, O. Rogojanu, G. A. Sawatzky, C. Ferrero, M. Borowski, O. Tjernberg, and N. B. Brookes, *Phys. Status Solidi B* **215**, 797 (1996).

<sup>14</sup>Y. Pontillon, A. Caneschi, D. Gatteschi, R. Sessoli, E. Ressouche, J. Schweitzer, and E. Levrieve-Berna, *J. Am. Chem. Soc.* **121**, 5342 (1999).

<sup>15</sup>Y. Furikawa, K. Kumagai, A. Lascialfari, S. Aldrovandi, F. Borsa, R. Sessoli, and D. Gatteschi (unpublished).

<sup>16</sup>M.-A. Arrio, P. Sainctavit, C. Cartier dit Moulin, C. Brouder, F. M. F. de Groot, T. Mallah, and M. Verdaguer, *Nucl. Instrum. Methods Phys. Res. B* **97**, 453 (1995).